Technical White Paper

STE/STQ Imaging

Li Shuangshuang Lan Bangxin

mindray 迈瑞

Healthcare within reach

Contents

STE/STQ Imaging

A New Solution to Ultrasound Elastography

Li Shuangshuang, Lan Bangxin

Preface

In the past two decades, methods of in vitro non-invasive detection of human tissue stiffness have been a great concern of researchers, and a variety of different elastography techniques have emerged around the world to try to obtain tissue stiffness information [1-4]. Ultrasound elastography expands the application scope of ultrasound diagnosis by adding stiffness information to conventional ultrasound diagnostic images. Now more and more doctors have confirmed that ultrasound elastography has great clinical significance in various application fields [4-11], especially in auxiliary diagnosis of liver fibrosis, liver cirrhosis, and certain cancers (such as breast cancer, thyroid cancer, and cervical cancer). With emergence of large-scale clinical multi-center studies and comparative studies one after another [12-14], the clinical application of ultrasound elastography is further improved, and the operation is increasingly standardized. Besides, change to tissue stiffness frequently occurs in the progress of many clinical diseases or tissue damage. Therefore, elastography has been continuously expanded to new clinical application fields such as muscle, gynecology, obstetrics, medical artificial intelligence, lung, prostate, and heart [15-21], showing great clinical potential and arousing the continued interest of researchers.

Ultrasound elastography is divided by technical principles into three categories: strain elastography, shear wave elastography based on acoustic radiation force, and transient elastography based on external vibration. Transient elastography must use a specially designed probe with a vibrator, and cannot provide elastic distribution images. It is mainly used for liver and is suitable for elastic detection of relatively uniform diffuse lesions. Strain elastography and shear wave elastography based on acoustic radiation force can not only use probes commonly used in conventional B-ultrasound examinations, but also provide elastic distribution images, which are convenient for observing the distribution of internal tissue stiffness. They are widely used for soft tissue examinations, and have become a hot spot in clinical research.

Ultrasound strain elastography provides real-time strain images within a region of interest (ROI), and has been widely used in clinical diagnosis for more than ten years. According to the Hooke's law, under the same pressure, the strain of stiff tissue is small, while the strain of soft tissue is large. Therefore, after applying uniform pressure through the probe, the strain distribution images of the tissue can reflect the elastic difference between different parts of the tissue. However, under different pressures, even the same tissue may exhibit different strain results. Therefore, to obtain stable and repeatable elastic image results, strain elastography has high requirements for clinical operation. In practical applications, doctors must be experienced in obtaining reliable images or judging soft and stiff tissues correctly.

In recent years, shear wave elastography has gained more clinical attention by providing quantitative tissue stiffness measurements. Quantitative measurement can greatly expand the clinical applications of elastography, and also make the development and research of

elastography reach a new climax. Shear wave elastography mainly displays shear wave transmission velocity or tissue elastic modulus, such as Young's modulus and shear modulus. Young's modulus is the most common indicator of tissue stiffness, and a higher Young's modulus value indicates a higher stiffness. For a linear, elastic, isotropic medium, the Young's modulus is calculated as:

$$E = 3G = 3\rho Cs^2$$

Where, G is the shear modulus; ρ is the density of the tissue; Cs is the transmission velocity of the shear wave. According to the formula, shear waves transmit faster in stiff tissues and slower in soft tissues [22-24].

Shear wave elastography has developed rapidly in recent years, but researchers still face many challenges, including how to obtain elastic images of improved quality and accuracy, how to obtain more stable and repeatable elastic measurement results, how to provide more clinical research analysis tools, and how to make the operation simpler and more convenient. Transrectal or transvaginal ultrasound intracavitary probe elastography techniques need particular concerns. Compared with linear array probes and convex array probes, requirements for small probe size and wide field of view increase technical and operation difficulties, resulting in very few ultrasound products commercially available on the market. To solve the problem, Mindray developed Resona R9, which is a new ultrasound elastography solution.

About STE/STQ Imaging

Acoustic Radiation Force and Shear Waves

Mindray Resona R9's STE/STQ imaging can quantitatively display tissue stiffness information in the ROI in real time. As shown in Figure 1, a probe, used for conventional ultrasound examination, transmits focused ultrasound within the power range of medical diagnostic ultrasound to the tissue. Based on the acoustic radiation force effect (ARF) [3, 23], shear waves are generated in the target area inside the tissue. Through the patented matrix emission focus control technology of the Resona R9 platform, a single emission can simultaneously generate a wide range of shear wave sources in the depth range of 0.2 mm to 30 mm. The system then tracks shear wave transmission, and continuously detects and records tissue displacement changes caused by shear wave transmission in the ROI. Finally, through a series of calculations, the transmission velocity of shear waves is obtained, and then parameters such as the elastic modulus of the tissue are deduced [25]. To form a complete elastic image, the system may need to generate shear waves at several different locations.

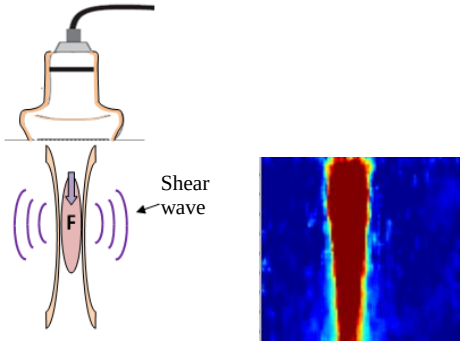

Figure 1: ARF and shear wave

Ultra-wide Beam Tracking Imaging

Due to the limitation that only a few ultrasound beams can be received after a single ultrasound transmission, conventional ultrasound systems often can only acquire tissue information in a very narrow area at one time. In shear wave elastography, the system needs to acquire a large number of echo signals in as large an area as possible in a very short period of time (within tens to hundreds of microseconds), so that the transmission position of shear waves at each moment can be more accurately located. In this way, the system can calculate the transmission velocity

of the shear waves more accurately.

Resona R9's STE/STQ imaging is based on the new ultra-wide beam tracking imaging technology, which can receive and process all signals in the range of 0.2 mm to 55 mm in real time after each ultrasound transmission, as shown in Figure 2(a). Therefore, STE/STQ can efficiently detect all necessary shear wave information in the ROI at frame rates up to 10,000 FPS, as shown in Figure 2(b). Besides, since the amplitude of shear wave generated by ARF is weak (usually only a few microns to tens of microns), STE/STQ can continuously fine-tune the position of the received beam with the transmission of the shear waves, to concentrate the energy of the ultrasound beam as much as possible and further improve the quality of received signals.

Figure 2(c) shows the transmission positions of shear waves captured in real time by Resona R9 at four different times. According to the figure, when the transmission velocities of shear waves at different depths are different, the wavefronts of shear waves at different depths are no longer consistent. The transmission velocity of the shear wave in the middle depth range is significantly faster, indicating that the tissue stiffness is higher in the middle depth range. This acceleration trend becomes more obvious as the shear wave gradually transmits into a larger region of high stiffness. In regions of uniform stiffness, the wavefront of shear waves is always stable. STE/STQ records the propagation process of shear waves in an ultra-fast, accurate, and complete manner.

This technique can acquire all necessary information in the entire ROI within tens of milliseconds, enabling real-time quantitative imaging of tissue elasticity. On the one hand, the ultra-fast signal capture can minimize the noise caused by other movements such as breathing and heartbeat during diagnosis. On the other hand, with better focused ultrasound beams, penetration can be improved.

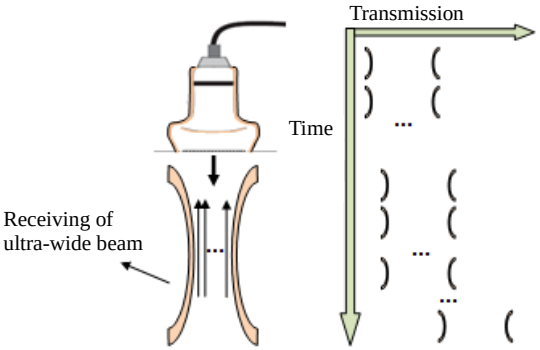

Figure 2(a): Ultra-wide beam tracking imaging

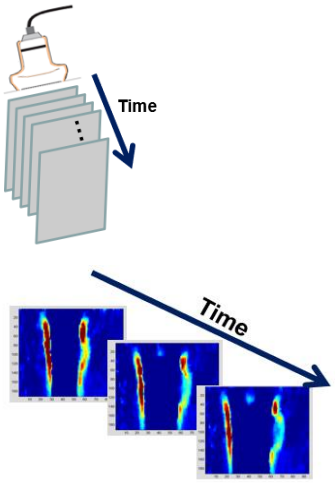

Figure 2(b): Detection frame rates up to 10,000 FPS

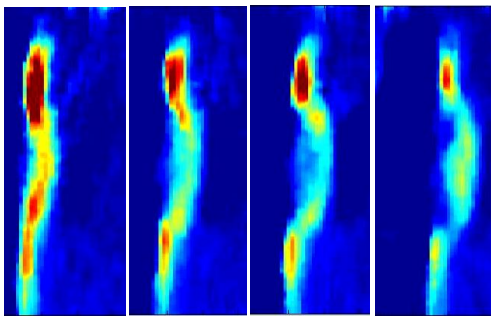

Figure 2(c): Capture transmission position of shear waves at different times accurately

STE/STQ Imaging Features

Resona R9 provides two types of shear wave elastography, both having their distinct features.

One is Sound Touch Elastography (STE). STE can perform two-dimensional color imaging on tissue stiffness information in a large ROI, display the elastic distribution of the lesions, and further measure the elasticity value as needed. STE not only shows details of tissue elasticity distribution more intuitively through the elasticity images, but also provides the local quantitative elasticity value of the tissue through the measurement results.

STE can provide a variety of quantitative elastic maps for different clinical applications for users to choose, as shown in Figure 3. In the figure, Cs is the shear wave velocity, in m/s; G is the shear modulus, in kPa; E is the Young's modulus, in kPa. Note that, although the unit of shear modulus G and Young's modulus E are the same, their physical meanings are completely different, and there may be up to several times of difference between the values. The quantitative results obtained clinically cannot be used for numerical comparison directly. For isotropic elastic tissues, the formula E = 3G can be approximated for comparison.

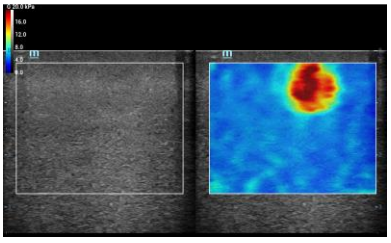

Figure 3: Quantitative elasticity diagram

HQE

STE supports two display modes. In most diagnostic scenarios, the real-time imaging mode can be used to display elasticity images continuously. For diagnosis of larger, stiffer, or deeper lesions, the high-quality imaging HQE mode can be used to improve the penetration of shear waves. In this mode, only a single frame of shear wave elasticity image is displayed at a time. As shown in Figure 4, HQE images can show the shape of deep lesions better, and images in a deep ROI (> 4 cm) have less noise.

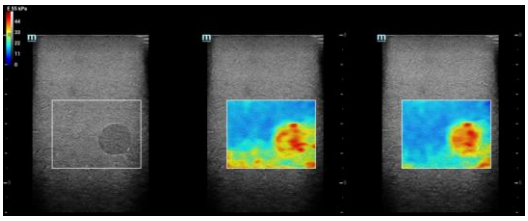

(a) (b) (c)

Figure 4: HQE. (a) B image; (b) HQE off; (c) HQE on

STE-HiRE High Resolution Shear Wave Elasticity

Due to the scale effect of existing shear wave elastography techniques, it is difficult to identify small lesions in the early stage. The latest Resona R9 offers the "Sharp Eye" technology, that is, the STE-HiRE mode, for higher resolution elasticity detection in small lesions. By focusing more precisely on the area near the target lesion, the shear wave is generated, and the acoustic wave energy is concentrated to detect only the shear wave transmission process in a small target area, thereby reducing the scale effect (the smaller the target scale, the larger the deviation of the measured value from the true value). The STE-HiRE mode can maximize the strength of the shear wave source and the signal-to-noise ratio (SNR) of the ultrasound echo signal. It can not only significantly improve the accuracy of elasticity measurement of small lesions, but also support multiple magnification display, which is convenient for users to locate the lesion boundary more accurately during measurement. As shown in Figures 5a, 5b, and 6, the STE-HiRE mode can accurately identify and measure soft or

stiff small lesions. The resolution of shear wave elasticity of linear array probes and intracavitary probe is 1 mm, and 2-3 mm respectively.

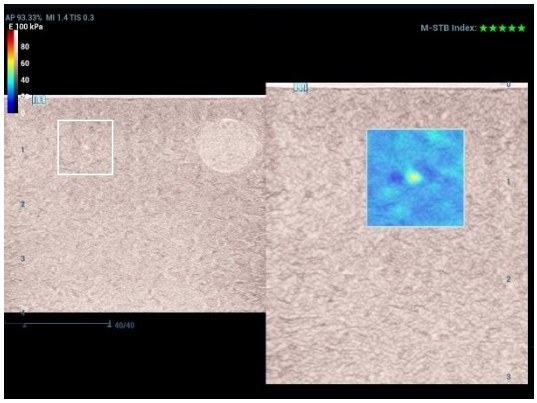

(a)

(b)

Figure 5 Linear array high-resolution shear wave. (a) 1 mm target elastic image (b) Target size measurement

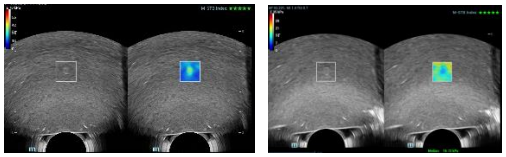

(a) (b)

Figure 6 Intracavitary high-resolution shear wave. (a) Stiff target (b) Soft target

Compared with the conventional STE mode, the scale effect of the STE-HiRE mode is significantly reduced. It can be used to observe the local boundary of the lesion more clearly, improve the accuracy and reliability of the local measurement value, and provide more details, as shown in Figure 7.

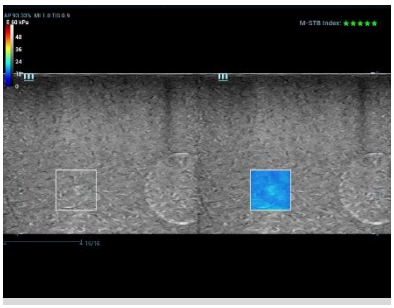

(a)

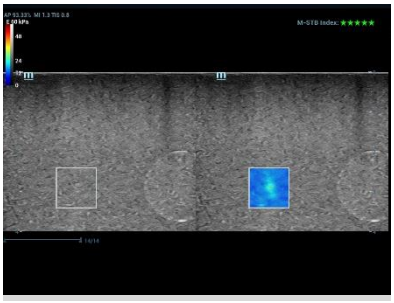

(b)

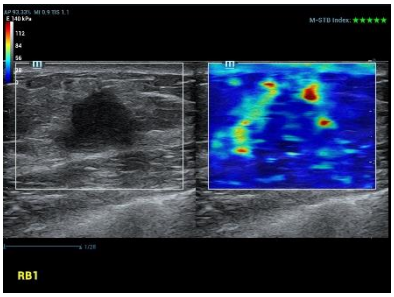

(c)

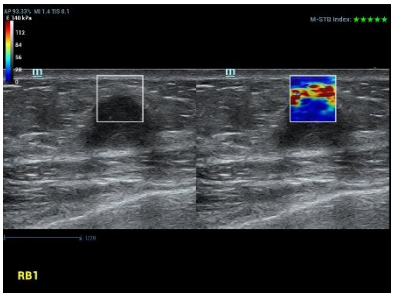

(d)

Figure 7: (a) Detection of 2 mm target in the conventional STE mode (b) Detection of 2 mm target in the STE-HiRE mode (c) Breast cancer manifestations in the conventional STE mode (d) Breast cancer manifestations in the STE-HiRE mode

STQ

Sound Touch Quantification (STQ) can directly quantitatively measure tissue stiffness within the ROI. STQ shows directly the tissue elasticity value in the ROI, which simplifies

and accelerates the quantitative measurement process, as shown in Figure 8. STQ further provides an elasticity result coordinate window, which can record the results of multiple consecutive measurements. Each measurement result corresponds to a bar graph on the time axis, and the height of the bar graph represents the mean elasticity value within the ROI obtained for that measurement. This window visually displays whether the multiple measurement results are stable.

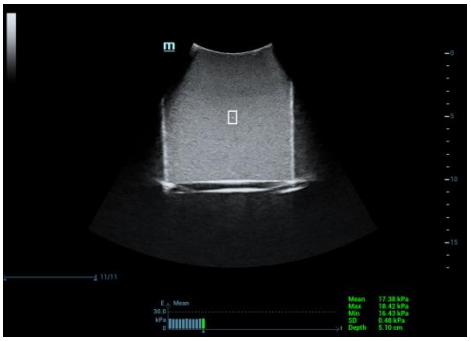

Figure 8: STQ display interface, phantom with uniform stiffness

STQ also provides inter-frame joint statistics function. After obtaining measurement results of multiple consecutive frames, users only need to select the number of frames to be counted through the "E Mean" knob, and then select the target frames to be counted on the elasticity result coordinate window. Then, the joint statistical results of selected multiple target frames can be automatically obtained, such as median and interquartile range (IQR), are shown in Figure 9. Users can also select the elasticity average (Emean) or the maximum elasticity (Emax) in the ROI according to different clinical examination applications, and perform "E Mean" automatic multi-frame statistics respectively. The inter-frame joint statistics function can further improve the accuracy of elasticity measurement results.

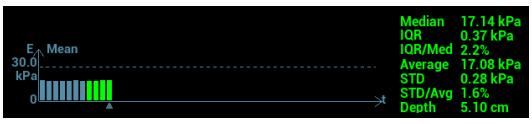

Figure 9 Inter-frame joint statistics function, where the number of statistical frames is 4, and the Emean in the ROI is the statistical target.

STE FIXED ROI

The latest Resona R9 also supports the inter-frame joint statistics function in the STE mode, which is called as STE FIXED ROI, as shown in Figure 10. In some clinical application scenarios, such as auxiliary diagnosis of liver fibrosis, if users want to make professional judgments intuitively based on the elasticity distribution images at fixed ROI size and depth while making multiple measurements conveniently, STE FIXED ROI can be used as a preferred rapid detection method to help doctors improve the detection efficiency.

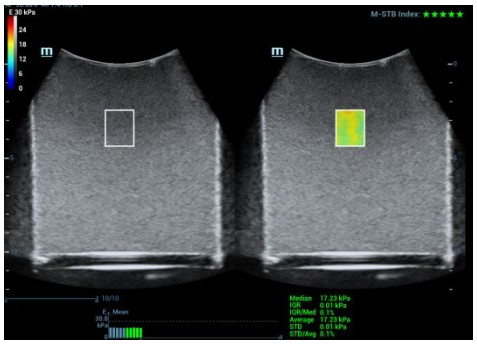

Figure 10: Inter-frame joint statistics function in the STE mode

STE/STQ Imaging Quality Control

Motion Stability

Since the amplitude of shear waves generated in human tissue is usually very weak, shear wave elastography is often sensitive to large motion disturbances in the examination. Especially during liver examinations, patients are usually required to hold their breath. To obtain stable and high-quality images, STE/STQ also provides a motion stability index (M-STB Index) to help doctors monitor the degree of motion disturbance in real time. As shown in Figure 11, the M-STB Index is

displayed in real time. When the motion disturbance is too large, the M-STB Index prompt is red; when the motion disturbance is small or not existing, the M-STB Index prompt is green; the smaller the motion disturbance, the more the green stars. When the M-STB Index of several consecutive frames is green, the shear wave elasticity images are collected in a stable state; when the M-STB Index is red, the shear wave elasticity images are collected in a moving state and the results may not be accurate.

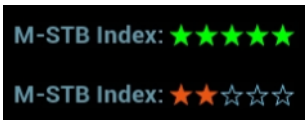

Figure 11: Motion disturbance prompt

Reliability Map

By comprehensively judging SNR of the echo signal, the strength of the shear wave and the current motion stability, Resona R9 also provides a reliability map (RLB Map), a reliability index (RLB Index) and a reliability view (RLB View) to assist doctors in judging the reliability area of the image and the reliability of the image. As shown in Figures 12a, 12b, and 12c, RLB Map reflects the reliable and unreliable areas of the data results in the shear wave image in real time. Areas with high reliability are shown in green, and areas with low reliability are shown in purple. RLB Index shows the reliability degree of the current shear wave image in percentage in three levels and colors, which represent the percentage of the reliable area in the entire ROI. Red indicates unqualified reliability, white indicates qualified reliability, and yellow indicates uncertain reliability, which requires doctors to make judgments based on experience. RLB Map is purple in the following cases: the motion RLB-Index is red; the probe is in poor contact; the shear wave measurement area contains noise or blood vessels.

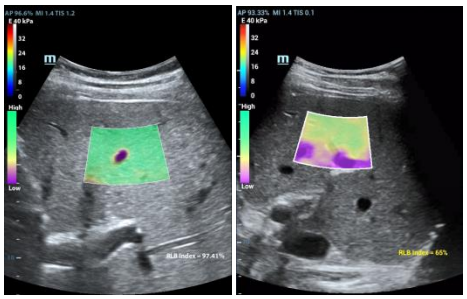

(a) (b)

(c)

Figure 12 RLB Map and RLB Index (a) RLB Map with blood vessels; (b) RLB Map in the moving state; (c) RLB Index

Reliability Area Elasticity Display

To facilitate the view and eliminate the interference of unreliable areas, users can also enable RLB View to display only the shear waves in the reliable area. Users only need to observe the shear wave images, and judge the quality of the shear wave images by the completeness. As shown in Figure 13a, when the motion stability is poor, the elasticity image completeness of the reliable region is low. As shown in Figure 13b, the vascular area within the ROI is also hollowed out. During measurement, the hollowed-out area is not included in the calculation.

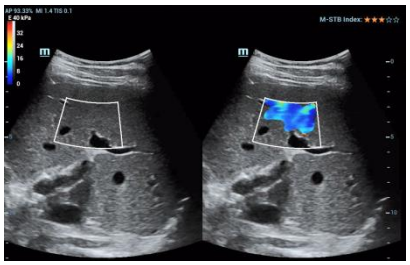

(a)

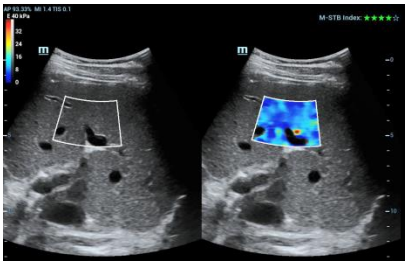

(b)

Figure 13: Reliability area elasticity. (a) Reliability area elasticity in the motion state; (b) Elasticity of reliability area with blood vessels

STE Multimodal Imaging (M-Reference)

M-Ref. *C&E*

Many studies show that, STE/STQ has shown excellent sensitivity and specificity in the clinical auxiliary diagnosis of various diseases by obtaining the Young's modulus of tissues. In actual clinical diagnosis, generally, tissue elasticity is not the only evidence. Doctors also need to analyze the micro-circulation perfusion characteristics of the lesions through the contrast-enhanced ultrasound imaging technology, and finally make a comprehensive judgment and analysis. However, due to the long operation time and the difficulty in holding the probe at the same scan section, in actual clinical practice, it is usually difficult to obtain the contrast-enhanced ultrasound imaging results and the shear wave elastography results at the same scan section.

To solve this problem, the latest Resona R9 provides the M-Reference imaging functions.

One of these functions is M-Ref. *C&E*. In this mode, a contrast-enhanced ultrasound image is selected from a video, usually an image with ultrasonic contrast agent mostly perfused, and the system automatically prompts the real-time matching between tissue image of the selected contras-enhanced ultrasound image and real time B images of the shear wave elastography. Users can obtain contrast-enhanced ultrasound images and shear wave elasticity images of the same scan section in turn, compare and display them on the same screen, and perform simultaneous quantitative measurement to obtain the contrast intensity information and the tissue stiffness information of the same area. Malignant tumors are often accompanied by changes in tissue stiffness and blood supply richness. M-Ref. *C&E* provides an effective tool for observing the changes between the two under the same scan section and guiding correlation research. Figures 14a, 14b, and 14c are the four-window on-screen display of the *C&E* function, the dual-window mixed display (MIX), and examples of low similarity in scan section matching, respectively.

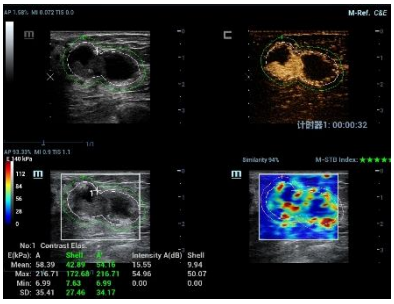

(a)

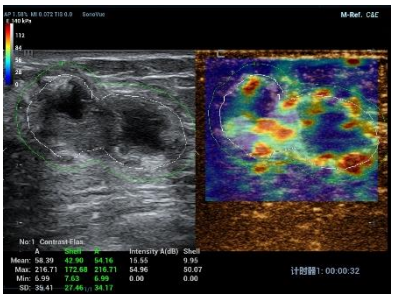

(b)

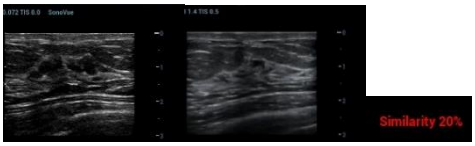

(c)

Contrast (tissue) STE(B)

Figure 14 *C&E* imaging. (a) Four-window on-screen display (b) Mixed display (c) tissue image of contrast-enhanced ultrasound imaging and B map of shear wave elastography in different scan section results low similarity notification

M-Ref. *E Compare*

Another function is the dual-modality imaging

of strain and shear wave elastography(named as M-Ref. E Compare). Strain elastography features high resolution and clear identification of lesion boundaries, but can only make qualitative judgments on the degree of tissue softness and stiffness. Shear wave elastography can quantitatively measure the elastic physical quantity of lesions, which has the advantages of quantitative statistical analysis, but the spatial resolution and lesion contour demarcation are unsatisfactory. Both technologies have been clinically proven tobe valuable, but are difficult to replace each other. As shown in Figure 15, By synchronously detecting and simultaneously displaying two types of elasticity imaging results in the same scan section, M-Ref. E Compare provides users with richer and more comprehensive stiffness information for improving the doctor's confidence and accuracy in diagnosis.

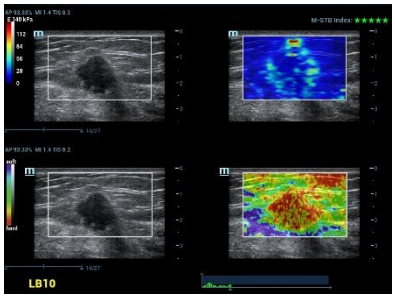

Figure 15 *M-Ref. E Compare*

STE Quantitative Tool

STE provides a variety of effective post-processing measurement tools for analysis of elasticity results. These measurement tools are easy to operate. For example, after the "Sync" function is enabled, users only need to trace the target area based on the B-mode image, and the system will automatically map it to the same position on the elastic image, as shown in Figure 16. This helps users to better identify lesion boundaries.

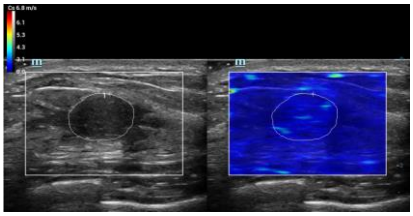

Figure 16: Sync function

Shell Quantitative Tool Kit

A unique feature of Mindray ultrasound system, the shell quantitative tool kit provides the elasticity values of both the lesion and the surrounding area (shell area) of the lesion, thus indicating the degree of infiltration of malignant tumor cells to the surrounding tissue, which has a great reference significance in the differentiation of benign and malignant masses. As shown in Figure 17, after users draw the lesion boundary, according to the selected thickness of the shell area, the system calculates and displays the elasticity results of both the lesion area and the shell area. The shell area can be either in the outside or inside of the lesion area.

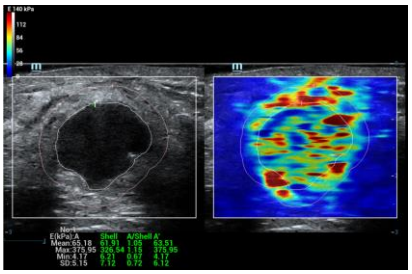

Figure 17: Shell quantitative tool kit

The elasticity histogram function can statistically display the color distribution of elastic images. Of course, the statistical results of the lesion area and its shell area can also be displayed on the same histogram to facilitate comparative analysis, as shown in Figure 18.

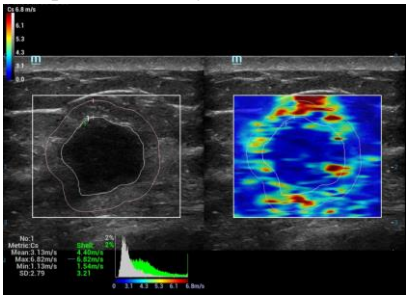

Figure 18: Elasticity histogram of the shell tool kit

Resona R9 also allows you to edit the shell. The thickness of the shell generated by the system is uniform by default. In a few cases, users need to correct the local boundary of the shell. As shown in Figure 19a, the shell area generated by default contains some normal muscle tissue, which is not the area that users want to measure. In this case, users can enable the shell editing function to correct part of the shell boundary to obtain new measurement result, as shown in Figure 19b.

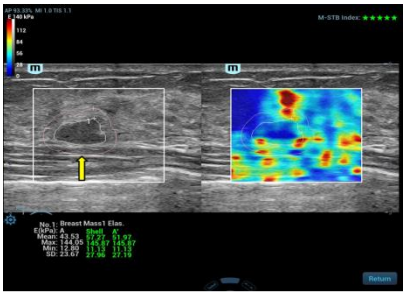

(a)

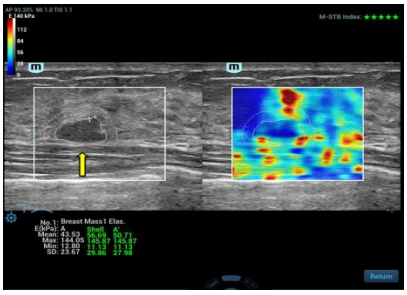

(b)

Figure 19: Shell editing function (a) Before shell edited (b) After shell edited

Trace-Auto Function

The latest Resona R9 also provides the Trace-Auto function. In breast applications, due to irregular shape of most breast lesions, doctors often need to spend a long time to manually trace the lesion tissue, and there are subjective differences among doctors. The Trace-Auto function allows the system to quickly outline and quantitatively measure the lesions automatically, improving the operation speed and the measurement stability. As shown in Figure 20, after Trace-Auto is enabled, users can select a starting point outside the lesion, move the trackball so that the complete lesion is included in the range of the green frame and the cross mark is in the center of the lesion, and then confirm the selection. The system can automatically trace the lesion and obtain quantitative measurement results of the lesion.

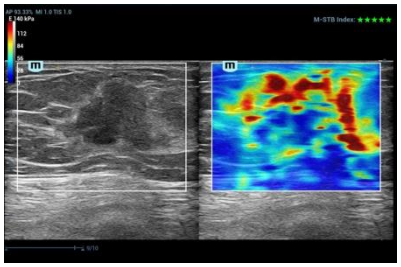

(a)

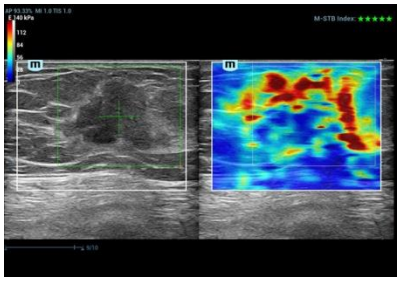

(b)

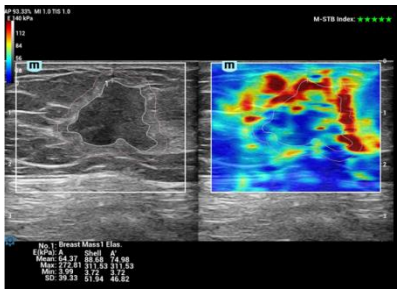

(c)

Figure 20: Trace-Auto

Elasticity Ratio

The elasticity of different target areas can be analyzed separately. The elasticity ratio indicates the ratio of elasticities of two areas, as shown in Figure 21.

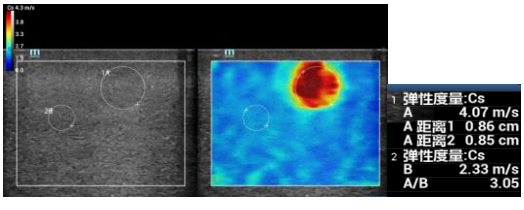

Figure 21: Elasticity ratio

In particular, for highly anisotropic tissues,

such as muscle tissue, Mindray STE has designed a unique "direction ratio" analysis tool for clinical use. Anisotropy makes shear wave transmission velocities vary greatly in different anatomical planes of the muscle. The degree of anisotropy changes with the tissue properties. As shown in Figure 22, after obtaining the elasticity images of different anatomical sections, the "direction ratio" function can measure and calculate the ratio of the elasticity results of different anatomical sections to indicate the degree of tissue anisotropy.

Figure 22: Biceps direction ratio calculation

All STE/STQ measurement results are recorded in the examination report. You can make statistics on the results of repeated measurements in the report. The elasticity data in the report can be easily exported as a separate file.

Cases study

Breast Application

One of the most mature and common applications of ultrasound elastography is auxiliary identification of benign and malignant breast cancers. Many clinical studies have proven that STE has excellent sensitivity and specificity in auxiliary diagnosis of breast cancers [26-30], and has high repeatability [31].

Doctors from a famous hospital in Shanghai used Mindray Resona 7 STE to conduct a clinical research on more than 100 breast patients. Pathological examinations were performed on 82 patients, of which 32 were malignant and 50 were benign.

The results show that STE can provide reliable and rich information to help distinguish benign from malignant tumors.

Elasticity images of most malignant tumors show high stiffness. Figure 23 is the STE elasticity result of a malignant lesion. The image of the breast lesion area is displayed in red, and the Young's modulus value of the surrounding tissue exceeds 100 kPa. The figure shows that the area of the high-stiffness area on the STE image exceeds the lesion area displayed on the B-mode image.

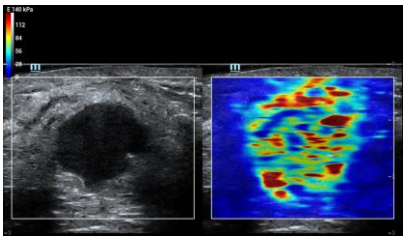

Figure 23: Elasticity images of malignant tumors show high stiffness

In clinical practice, the shear wave images of most breast malignant tumors show stiff rim signs (that is, the high hardness of the shell area). Figure 24a shows the image of an invasive ductal carcinoma of the breast, and its shell area is displayed in red, indicating that the tissue stiffness of the shell area is much higher than that of normal tissue. According to the map, the Young's modulus of the shell area exceeds 100 kPa, while the Young's modulus of normal tissue is lower than 40 kPa. The elasticity and shape of the shell area vary with the type and shape of the lesion, but the characteristics of high stiffness in the shell area mostly remain unchanged. Figure 24b shows the examination results of a case of breast carcinoma in situ. The maximum Young's modulus of the shell area is above 75 kPa, while the Young's modulus of normal tissue is below 20 kPa. Figure 24c shows the examination results of a case of breast carcinoma in situ with small foci of micro-invasion. The maximum Young's modulus of the shell area is above 250 kPa,

while the Young's modulus of normal tissue is below 20 kPa. Among 22 cases of breast cancer examined, 20 cases showed stiff ring signs, which may become a clear and valid feature for distinguishing benign from malignant lesions.

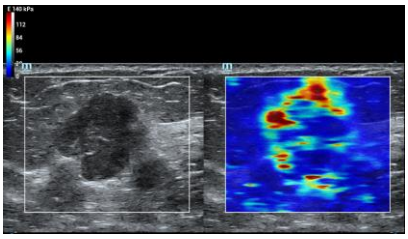
(a)

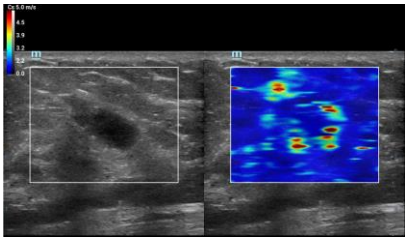
(b)

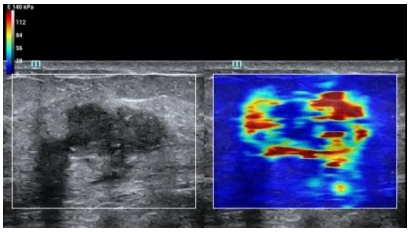
(c)

Figure 24: Stiff rim signs (high stiffness in the shell area) (a) Invasive ductal carcinoma; (b) Breast carcinoma in situ; (c) Breast carcinoma in situ with small foci of micro-invasion

In contrast, the stiffness of most benign breast lesions is similar to that of normal tissue or only slightly higher than that of surrounding normal tissue. The mean Young's modulus values in and around the lesion are often lower than 24 kPa. In some cases, the maximum Young's modulus values are close to 60 kPa in some areas within the lesion, while the mean value is still low. Figure 25a: Adenopathy of the breast; Figure 25b: Intraductal papilloma of the breast; Figure 25c: Fibroadenoma of the breast.

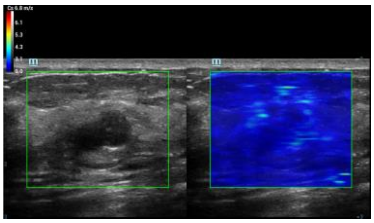
(a)

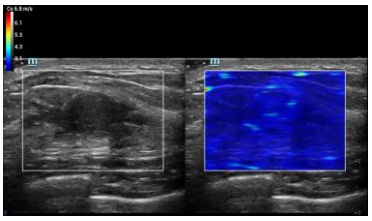
(b)

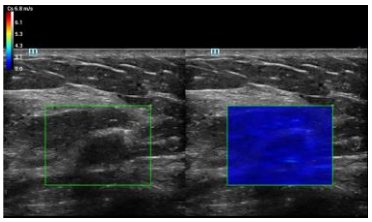
(c)

Figure 25: Images of (a) Adenopathy of the breast; (b) Intraductal papilloma of the breast; (c) Fibroadenoma of the breast.

In a clinical study, we recorded the mean and maximum values of Young's modulus in the shell area of 41 patients, the width of the shell is 3 mm, and the results are shown in Figure 26 and Figure 27. These results indicate that the maximum and mean values of Young's modulus in the shell area of most malignant tumors obtained by STE are higher than those of benign tumors. The average value of maximum Young's modulus in the shell area of malignant tumors is about 165 kPa (distributed between 50 kPa and 300 kPa), while that of benign tumors is about 64 kPa (distributed between 10 kPa and 110 kPa). The average value of mean Young's modulus in the shell area of malignant tumors is about 31 kPa (distributed between 10 kPa and 63 kPa), while that of benign tumors is about 16 kPa (distributed between 3 kPa and 30 kPa).

If 98 kPa is used as the cutoff value for distinguishing benign and malignant breast tumors, the sensitivity and specificity of the 3 mm shell max result in distinguishing benign

and malignant of the above lesions can reach 85% and 95%, and the area under the receiver operating characteristic curve (AUROC) can reach 0.90. The accuracy of critical value and ROC increases with the number of samples. Cutoff values may change with the shell thicknesses or measuring observation targets (for example, when shell mean is used).

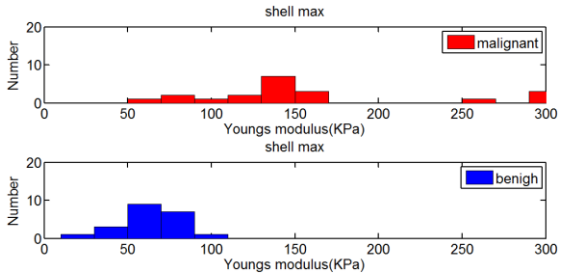

Figure 26: Maximum Young's modulus in the shell area

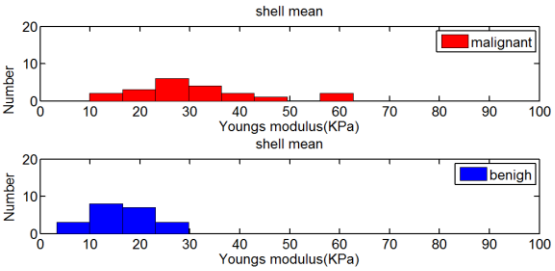

Figure 27: Mean Young's modulus in the shell area

The research shows that in routine breast ultrasound examination, STE/STQ after 2D gray-scale ultrasound examination can further improve the doctor's confidence in diagnosis. Especially when the BIRADS grade is 4a or above, needle biopsy is recommended. If it can be supplemented by shear wave elasticity examination, it is hoped that many unnecessary needle biopsies can be reduced. Figure 28 shows a case with a BIRADS grade of 4a, and its STE results suggest that it is more likely to be a benign lesion, which is confirmed as a fibroadenoma by pathological examination. If the BIRADS grade is downgraded from 4a to 3 based on the results of the STE images, the patient could be exempted from needle biopsy.

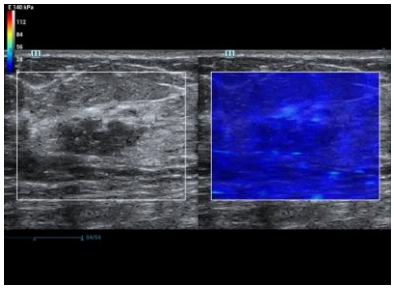

Figure 28: Breast fibroadenoma. with BIRADS grade of 4A, indicates as a benign lesion on the STE image

Liver Application

The liver is an important organ. Serious liver disorder often causes fatal consequences to the human body. However, most chronic liver diseases are often insidious and easily ignored, resulting in irreversible consequences. Early detection of liver lesions and the monitoring and management of chronic liver diseases are research hot spots in clinical practice. Liver fibrosis is the most common clinical pathological phenomenon caused by various chronic liver damage, with a high incidence. It may be caused by hepatitis B virus, hepatitis C virus, alcohol, fatty liver, drug damage, and other factors. Persistent liver fibrosis may develop into life-threatening major diseases such as liver cirrhosis and liver cancer. The progression of liver fibrosis can lead to an increase in liver stiffness, so the detection of liver stiffness has become an important means of liver fibrosis assessment. Many clinical studies have proven that STE has excellent sensitivity and specificity in early diagnosis of liver fibrosis, and has high repeatability [13, 32-37].

Resona 7 STE/STQ has also shown important value in the non-invasive detection of hepatic fibrosis in clinical applications. Figure 29 shows typical STE results of patients without hepatic fibrosis, patients with marked hepatic fibrosis, and patients with liver cirrhosis. According to the figure, as the degree of

hepatic fibrosis increases, the color of the STE image changes significantly, and the measured elasticity value also increases. With the quantitative scale preset by the system, for livers without hepatic fibrosis or with mild hepatic fibrosis, STE images are displayed in blue evenly. For livers with marked or severe hepatic fibrosis, STE images usually show a large amount of cyan. For liver cirrhosis, STE images are mainly yellow and red.

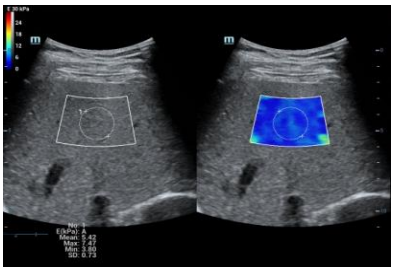

(a)

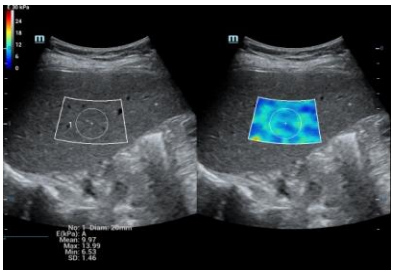

(b)

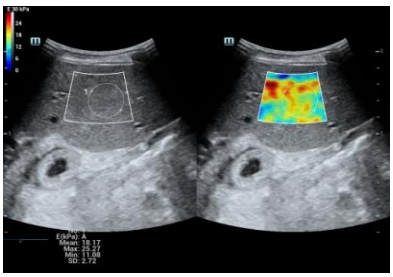

(c)

Figure 29: STE images of different degrees of hepatic fibrosis (a) No hepatic fibrosis; (b) Serious hepatic fibrosis; (c) Liver cirrhosis

Doctors from the liver disease center of a famous hospital in Shanghai used Mindray Resona 7 STE to conduct a clinical research on more than 300 patients with liver diseases, including HBV, HCV, DILI, and AIH. Liver biopsy was performed on 209 patients, including 88 patients with HBV.

Liver STE is generally performed from the right intercostal space and the STE measured value often fluctuates slightly due to impact of the probe contact surface size and the patient breathing. Therefore, it is generally recommended to select the mean value in a circular measurement area with a diameter of ≥ 10 mm as the single measurement result. It is also recommended to repeat the measurement 3-10 times, and then take the median or mean value of multiple measurements as the final measurement result to improve the accuracy and repeatability of liver STE measurement. To reduce impact of the patient's breathing on the STE measured value, patients should hold their breath before and during of liver STE to keep the motion stability for 4-5 stars.

In this clinical study, we selected the E mean value in a circular measurement area with a diameter of 20 mm, and took the median of the measurement values of 5 times as the final result. Pathological examination was based on the Scheuer scoring system to evaluate the staging results of liver fibrosis.

The research results show that STE/STQ has great clinical significance in assisting non-invasive diagnosis of early liver cirrhosis and staging of liver fibrosis. With the progress of liver fibrosis, the measured value of STE also increases. The Young's modulus of most patients with cirrhosis is above 11.3 kPa; that of most patients with severe liver fibrosis is within the range of 9.5 kPa to 11.3 kPa, and that of most patients without liver fibrosis or only mild liver fibrosis is lower than 7.2 kPa or even 6.4 kPa.

Figure 30 shows the statistical results of the Young's modulus values in the above-mentioned 209 cases according to different pathological Scheuer stage values. According to the figure, there is a great difference between the measured values of patients with different liver fibrosis stages. Taking patients with stage of ≥ S4 and ≤S3 as an example, the patient's AUROC can reach

0.95.

In addition, considering the possible differences between different pathogenic factors, the Young's modulus values of the livers of 88 HBV cases were observed separately, and it was found that the STE measured results also increased with the progress of liver fibrosis, as shown in Figure 31.

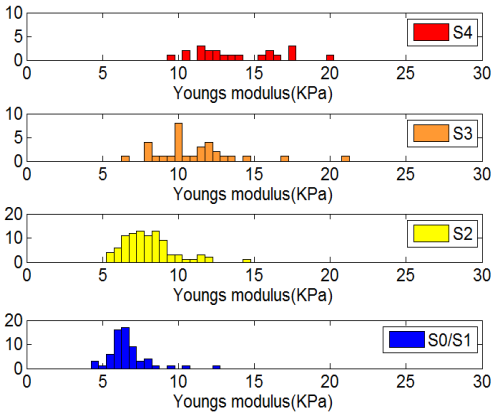

Figure 30 Distribution of Young's modulus values in different stages of liver fibrosis

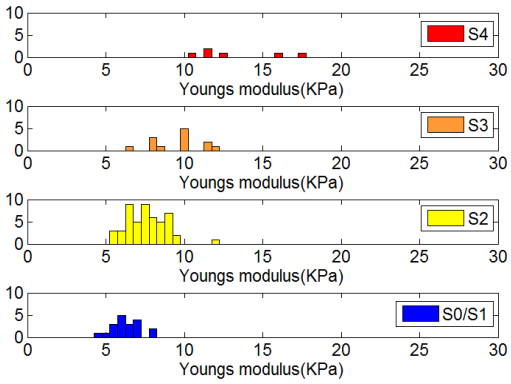

Figure 31. Distribution of Young's modulus values in different fibrosis stages - HBV cases

Prostate Application

The incidence and mortality of prostate cancers are increasing around the world. Gleason score of systematic biopsy are usually considered as the gold standard of prostate cancers. However, since prostate cancers are not obviously indicated by conventional ultrasound examinations and multifocal prostate cancers are common, systematic biopsy is not satisfactory due to its low detection rate and missed diagnosis of significant prostate cancers. Prostate cancers are often accompanied by increased prostate stiffness as the glands with prostate cancer damage their structure and trigger wound repair, leading to stroma and collagen deposition. Therefore, researches on the diagnostic efficacy of shear wave elasticity for prostate cancers and the targeted biopsy guided by shear wave elasticity are also hot spots in recent years.

In a latest clinical application for prostate, Resona R9's STE also showed potential clinical value in non-invasive diagnosis of prostate cancers. Figure 32 shows a normal prostate. As shown in the cross section, the inner gland of the prostate is stiffer than the outer gland, and the boundary between the inner and outer glands is clear. Special image manifestations have been found in the study of prostate lesions. In Figure 33, Figure (a) is a case of benign prostatic hyperplasia (longitudinal section), and Figure (b) is a case of prostate cancer (longitudinal section). According to the figures, with the quantitative scale preset by the system, for benign prostatic hyperplasia, the boundary of the external gland area is clear, which is shown as a relatively uniform blue; for a prostate cancer, the stiffness of the external gland increases, which is displayed in red, and the measured Young's modulus is greater than 60 kPa.

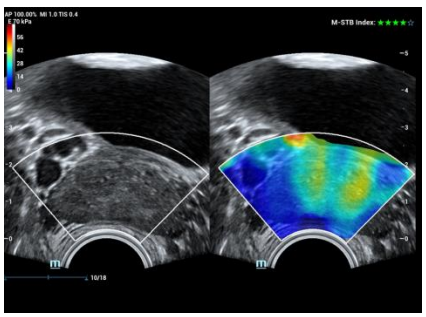

Figure 32 STE image of prostate cross section, using a conventional intracavitary probe

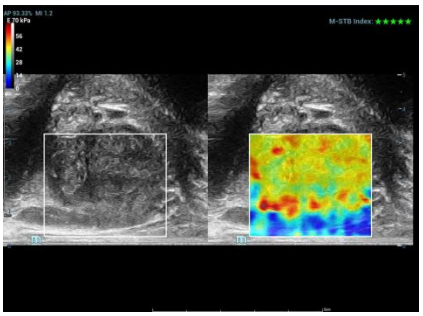

(a)

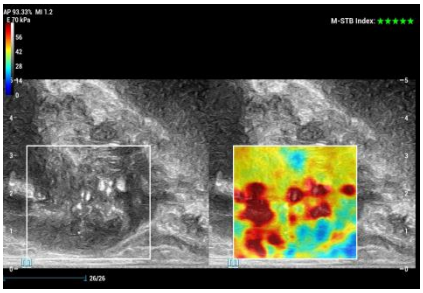

(b)

Figure 33 STE image of longitudinal section of prostate (a) Benign prostatic hyperplasia; (b) Prostate cancer; using a biplane transrectal probe

Doctors from a famous hospital in Shanghai used Mindray Resona R9 STE to conduct a clinical research on more than 100 prostate patients. STE is performed on multiple sections of the prostate using the linear array of Mindray's biplane probe. After STE, transperineal prostate systematic biopsy is then performed. It is required to use the same section for STE and systematic biopsy. When the Gleason score of biopsy result is equal to or greater than 6, prostate cancer is confirmed.

During prostate STE, the probe is generally kept still in the rectum, and the patients are required to keep still and hold their breath. Most prostate cancers are multifocal lesions in the external glands which are small. Users can manually select a circular measuring box with a diameter of 5 mm, and measure in the area with the highest measured value in the external gland area or perform tracing measurement on the entire external gland of the prostate. In clinical practice, it is often difficult to identify the external gland area and select the placement position of the local measurement frame. To solve the problem, the system also provides a prostates automatic measurement toolkit. The toolkit can automatically identify and indicate the external gland area during scanning, automatically optimize the position of the ROI in the elasticity image, and automatically place the local measurement circle to obtain the elasticity quantitative result after obtaining an ideal image, as shown in Figure 34.

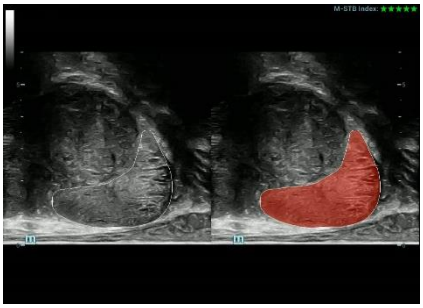

(a)

(b)

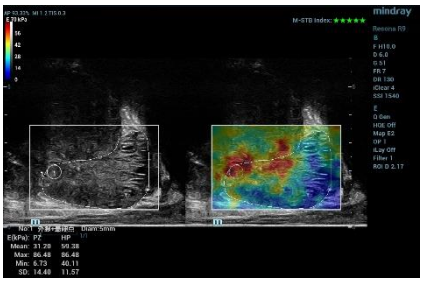

(c)

Figure 34 Prostate automatic measurement toolkit (a) Automatically identify the external gland area; (b) Automatically optimize the position of ROI in the elasticity image; (c) Automatically place the local measurement

circle to obtain elasticity quantitative results

During prostate STE using the biplane probe, as shown in Figure 35, the array of the biplane probe is at the side of the probe (different from the conventional intracavitory probe), and easily squeeze the prostate tissue, resulting in false positive cases. Even though the doctor holds the probe and does not apply any pressure to the prostate, the external gland has actually been squeezed, as shown by the red dotted line. Therefore, during prostate STE using the biplane probe, as shown in Figure 36, operator need to apply a force in the opposite direction to the probe to deflect the probe in the direction of the black probe, so as to reduce the force on the prostate and deformation of the prostate external gland, as shown by the red dotted line. It is also necessary to keep the probe to maintain its motion stability within the range of 4-5 stars during STE to ensure image quality.

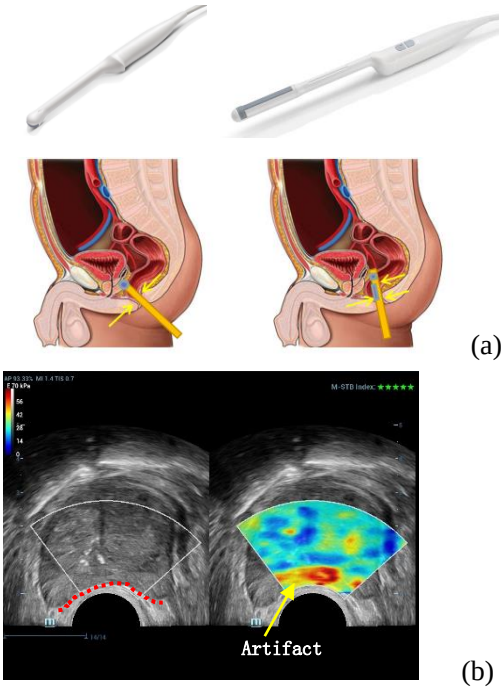

(a)

(b)

Figure 35 (a) Difference between biplane probe and conventional intracavitary probe (b) In the case of uncorrected pressure, the external glands in the STE image of the transverse section of the prostate have artifacts

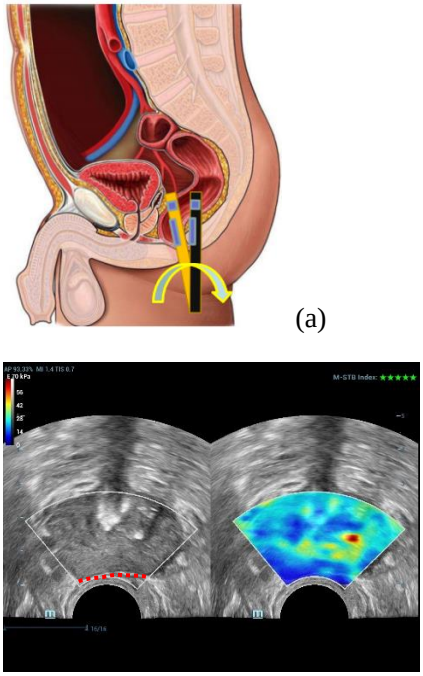

(a)

(b)

Figure 36 (a) The direction of pressure correction of the dual-plane probe (b) After pressure correction, the STE image of the transverse section of the prostate is normal

The research results show that STE/STQ has great clinical significance in assisting the diagnosis of prostate cancers. As shown in Figure 37, based on the Gleason grading standard, the patient's AUROC can reach 0.84, and the shear wave Young's modulus of prostate cancer is generally greater than 41 kPa. This clinical study also finds that, the higher the Gleason score, the greater the STE measured value.

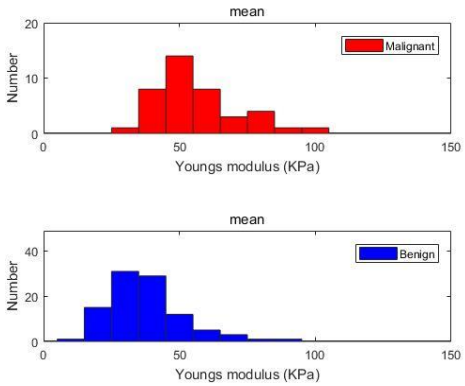

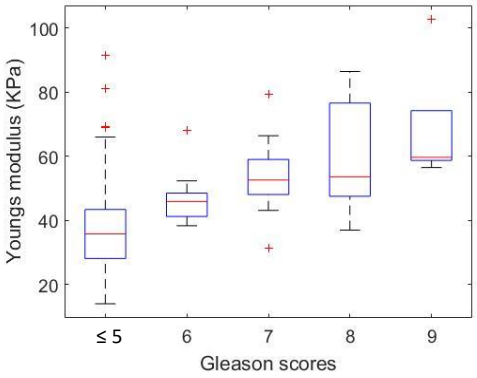

Figure 37 Young's modulus distribution of prostate cancer and benign prostate, and the change of prostate Young's modulus with Gleason grade

Note that although most prostate cancers are multifocal, there are also some cases with nodular manifestations. This clinical study further finds that, the STE measured value of malignant prostate nodules are higher than those of multifocal prostate cancer cases, and are also significantly higher than the prostate elasticity results of benign lesions, as shown in Figure 38.

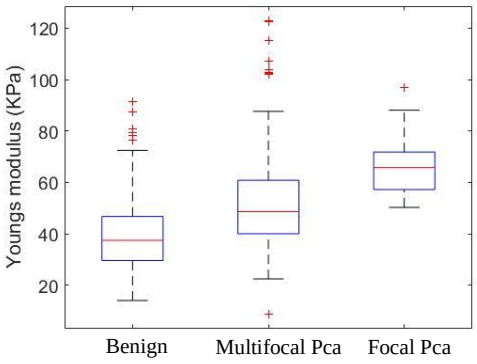

Figure 38. Young's modulus distribution of malignant prostate nodules and multifocal prostate cancer cases

Conclusion

Mindray STE/STQ provides a new method to quantitatively obtain tissue elasticity information for clinical ultrasound diagnosis. Based on the ultra-wide beam tracking imaging platform, STE/STQ can detect all necessary shear wave information in the ROI quickly at a frame rate of up to 10,000 FPS. By using improved focused ultrasonic beam, STE/STQ can reach an ultra-high detection frame rate, and have good penetration, so as to obtain elasticity images and measurement results better. The high-resolution STE-HiRE technology developed by Mindray can significantly improve the resolution and contrast of lesion boundaries, especially the detection accuracy and repeatability of small lesions.

In this clinical study, STE/STQ is first applied to the ultrasound diagnosis of breast cancer and liver fibrosis. Despite of a small clinical sample size, the research results have proven the reliability and effectiveness of STE/STQ in the above applications. In particular, it has been found in clinical practice that its unique shell analysis tool can provide more reliable clinical diagnostic information for the identification of benign and malignant breast tumors. Its unique inter-frame joint statistical function can greatly simplify the measurement process of liver fibrosis detection. In a latest clinical study, STE has also demonstrated its potential clinical value in the non-invasive auxiliary diagnosis of prostate cancers.

Currently, multiple hospitals are using STE/STQ to conduct more extensive clinical studies with larger sample sizes, including breast, liver, spleen, thyroid, prostate, muscle, nerve, skin, pediatrics, obstetrics, gynecology, and pelvic floor, and have explored the clinical operation quality control and operation specification of elastography. Many research results have shown that STE/STQ has shown excellent sensitivity and specificity in the clinical auxiliary diagnosis of various diseases [32-43].

Different clinical application sites, as well as cancer types, pathogenic causes, biochemical indicators, clinical interventions, and other factors may also have a certain impact on the

elasticity measured value. We hope that in the future that more comprehensive, accurate, and detailed clinical diagnosis reference index suggestions for more subdivided application parts will be offered, so as to better help clinical diagnosis. We have also noticed that in recent years, the development of medical AI technology [18, 44-45] has a profound impact on the accuracy and convenience of ultrasound diagnosis, and it will be important study direction of promoting the development of medical AI technology through extraction and application of tissue elasticity feature information.

References

[1] Ophir J, Cespedes I, Ponnekanti H, et al. Elastography: a quantitative method for imaging the elasticity of biological tissues. Ultrasonic Imaging, 1991, 13: 111-134.

[2] L. Gao, KJ Parker. Imaging of the elastic properties of tissue – a review. Ultrasound in Medicine and Biology. 1996, 22(8), 959-976

[3] Sarvazyan AP, Rudenko OV, Swanson SD, Fowlkes JB, EmelianovSY. Shear wave elasticity imaging: A new ultrasonic technology of medical diagnostic. Ultr. Med Biol 1998;20:1419 –1436.

[4] Giovanna F, et al. Liver ultrasound elastography: an update to the world federation for ultrasound in medicine and biology guidelines and recommendations. Ultrasound in Med & Biol, 2018; 00(00):1-22

[5] Richard G.B, Stephanie R.W, Deborah R, et al. Update to the society of Radiologists in ultrasound liver elastography consensus statement. Radiology, 2020; 00:1-12

[6] Chinese Society of Hepatology, Chinese Medical Association, et al. Consensus on the diagnosis and therapy of hepatic fibrosis. Clin Hepatol,2019;35(10):2163-2172

[7] Anke Thomas. Real-time sonoelastography performed in addition to B-mode ultrasound and mammography: improved differentiation of breast lesions? Academic Radiology. 2006;13(12):1496-1504

[8] Richard G.B. Breast Elastography: How to perform and integrate into a “Best-Practice” patient treatment algorithm. J Ultrasound Med. 2020; 39:7-17

[9] Lei Z, Zhimin D, Fajin D, et al. Diagnostic performance of multiple sound touch elastography for differentiating benign and malignant thyroid nodules. Front. Pharmacol. 9:1359

[10] Anke Thomas. ReaL-time sonoelastography of the cervix: tissue elasticity of the normal and abnormal cervix. Academic Radiology. 2007;14(2):193-200

[11] Jianqiao Zhou, Weiwei Zhan, et al. Stiffness of the surrounding tissue of breast lesions evaluated by ultrasound elastography. European Society of Radiology. 2014; DOI 10.1007/s00330-014-3152-7

[12] Lu-ying G, Yang G, Wen X, et al. Can combined screening of ultrasound and elastography improve breast cancer identification compared with MRI in women with dense breasts-a multicenter prospective study. 2020; 11(13):3903-3909

[13] Jinfen W, Manli W, et al. Usefulness of new shear wave elastography technique for noninvasive assessment of liverfibrosis in patients with chronic hepatitis B: a prospective multicenter study. Ultraschall in Med. 2021

[14] Leah A.G, Andrew T.T, Paula B, et al. Repeatability and agreement of shear wave speed measurements in phantoms and human livers across 6 ultrasound 2-dimensional shear wave elastography systems. Invest Radiol, 2020;55(4):191-199

[15] Xiao L, Hong-kui Y, Shu-ya S, et al. Quantitative evaluation of passive muscle stiffness by shear wave elastography in healthy individuals of different ages. European Radiology. 2020;31(5):3187-3194

[16] Bertrand G, et al. In vivo assessment of the levator ani muscles using shear wave elastography: a feasibility study in women. Int Urogynecol J. 2019;30(7):1179-1186

[17] Jimei S, Nan L, Wei J, et al. Clinical application of cervical shear wave elastography in predicting the risk of preterm delivery in DCDA twin pregnancy. BMC Pregnancy and Childbirth. 2022; 22:202

[18] Ruobing H, Zehui L, et al. AW3M: An auto-weighting and recovery framework for breast cancer diagnosis using multi-modal ultrasound. Med Image Anal. 2021;72:102137

[19] Gian Piero B, el al. "Elasto-lung point": A new tool for the sonographic confirmation of pneumothorax. Clin Respir J. 2020;14(8):758-762

[20] Thineskrishna A, Cheng W, et al. Characterisation of prostate lesions using transrectal shear wave elastography (SWE) ultrasound imaging: a systematic review. Cancers 2021;13:122

[21] Lana B.H.Keijzer, Mihai S, et al. Reproducibility of natural shear wave elastography measurements. Ultrasound in Med. &Biol. 2019;45(12):3172-3185

[22] JLGennisson,SCatheline, et al. Transient elastography in anisotropic medium: Application to the measurement of slow and fast shearwave speeds in muscles. J Acoustical Society of America. 2003;114:536-541

[23] M. L Palmeri., M. H Wang. Quantifying hepatic shear modulus in vivo using acoustic radiation force. Ultrasound in Med & Biol. 2008;34(4):546-558

[24] G R Torr. The acoustic radiation force. Am. J. Phys. 1984; 52(5)

[25] Joyce McLaughlin and Daniel Renzi. Shear wave speed recovery in transient elastography and supersonic imaging using propagating front. Inverse Problems.2006; 22:681–706

[26] Lei Z, Jinfeng X, Huaiyu W, et al. Screening breast lesions using shear modulus and its 1-mm shell in sound touch elastography. Ultrasound in Med & Biol.2019;45(3):710-719

[27] Leidan H, Mengke M, Zhen D. Gong X. Quantitative evaluation of tissue stiffness around lesion by sound touch elastography in the diagnosis of benign and malignant breast lesions. PLoS ONE.2019;14(7):e0219943

[28] Yan-jun X, Hui-ling G, et al. Role of "stiff rim" sign obtained by shear wave elastography in diagnosis and guiding therapy of breast cancer. 2021;18(15):3615-3623

[29] Xie X, Zhang Q, Liu S, Ma Y, et al. Value of quantitative sound touch elastography of tissues around breast lesion in the evaluation of malignancy. Clin Radiol.2021;76(1):79.e21-79.e28

[30] Ping X, Mei W, Min Y, et al. Evaluation of internal and shell stiffness in the differential diagnosis of breast non-mass lesions by shear wave elastography. World J Clin Cases 2020;8(12):2510-2519

[31] Lu Z, Yi-jie D, Jianqiao Z, et al. Similar reproducibility for strain and shear wave

elastography in breast mass evaluation: a prospective study using the same ultrasound system. Ultrasound in Med & Biol. 2020;46(4):981-991

[32] Ilias G, Petros D, Spyros Y, et al. Comparison of sound touch elastography, shear wave elastography and vibration-controlled transient elastography in chronic liver disease assessment using liver biopsy as the "Reference Standard". Ultrasound Med & Biol. 2020;46(4):959-971

[33] Lulu Y, Jiawu L, Lin M, et al. Noninvasive assessment of liver fibrosis in chronic hepatitis B carriers with sound touch elastography: study of surgical pathology specimens. Expert Rev Med Devices. 2020;17(8):845-853

[34] Lulu Y, Wenwu L, Du H, et al. Shear wave-based sound touch elastography in liver fibrosis assessment for patients with autoimmune liver diseases. Quant Imaging Med Surg. 2021;11(4):1532-1542

[35] Xinping Ren, Shujun Xia, Zhongxin Ni, et al. Analysis of three ultrasound elastography techniques for grading liver fibrosis in patients with chronic hepatitis B. Radiol Med. 2018;123(10):735-741

[36] Ruo-kun Li, Xin-pin Ren, Fu-hua Yan, et al. Liver fibrosis detection and staging: a comparative study of T1p MR imaging and 2D real-time shear-wave elastography. Abdom Radiol(NY). 2018;43(7):1713-1722

[37] Kun Huang, Qinyuan Li, Weimei Zeng, et al. Ultrasound score combined with liver stiffness measurement by sound touch elastography for staging liver fibrosis in patients with chronic hepatitis B: a clinical prospective study. Ann Transl Med. 2022;10(6):271

[38] Cheng C, Sirui L, Chenyang Z, Ruojiao W, et al. Activity of keloids evaluated by multimodal photoacoustic/ultrasonic imaging system. Photoacoustics.2021;24:100302

[39] Na X, Bei X, et al. Dual modal ultrasound elastography of the sternocleidomastoid muscle in healthy infants: a prospective study. Advanced Ultrasound in Diagnosis and Therapy.2019;04:182-186

[40] Fajin D, Huaiyu W, Lei Z, et al. Diagnostic performance of multimodal sound touch elastography for differentiating benign and malignant breast masses. J Ultrasound Med. 2019;38(8):2181-2190

[41] Jian Z, Manli W, Qingjuan W, et al. Liver and spleen stiffness measurements by sound touch elastography and sound touch quantification. Advanced Ultrasound in Diagnosis and Therapy.2020;04:315-321

[42] Junling G, Lei X, et al. A deep Siamese-based plantar fasciitis classification method using shear wave elastography. IEEE Access.2019,PP(99):1-1

[43] Yi Z, Shujun X, Xinping R, et al. A study of spleen shear-wave elastography in indirect prediction of liver fibrosis in patients with chronic hepatitis B. Clin Hemorheol Microcirc. 2020;76(1):63-72

[44] Zhong L, Huiying W, et al. Diagnosis of significant liver fibrosis in patients with chronic hepatitis Busing a deep learning-based data integration network. Hepatol Int. 2022

[45] Jian W, et al. Auto-weighting for breast cancer classification in multimodal ultrasound. MICCAI. 2020; 12266:190-199

Mindray Medical
WeChat Account

Customer Service Center
WeChat Account

Customer
service hotline 400 700 5652

www.mindray.com

mindray 迈瑞

Healthcare within reach